ORGANOMETALLICS
Article
pubs.acs.org/Organometallics

Photoelectron Spectroscopy of Palladium(I) Dimers with Bridging Allyl Ligands

Phuong Diem Dau,[†,‡] Damian P. Hruszkewycz,[§,‡] Dao-Ling Huang,[†] Matthew J. Chalkley,[§] Hong-Tao Liu,[†] Jennifer C. Green,*[,⊥] Nilay Hazari,*[,§] and Lai-Sheng Wang*[,†]

[†]The Department of Chemistry, Brown University, Providence, Rhode Island 02912, United States
[§]The Department of Chemistry, Yale University, P.O. Box 208107, New Haven, Connecticut 06520, United States
[⊥]The Inorganic Chemistry Laboratory, University of Oxford, South Parks Road, Oxford, OX1 3QR, U.K.

Ⓢ *Supporting Information*

ABSTRACT: The dianionic Pd^I dimers [TBA]$_2$[(TPPMS)$_2$Pd$_2$(μ-C$_3$H$_5$)$_2$] (**1**) [TBA = tetrabutylammonium, TPPMS = PPh$_2$(3-C$_6$H$_4$SO$_3$)$^-$] and [TBA]$_2$[(TPPMS)$_2$Pd$_2$(μ-C$_3$H$_5$)(μ-Cl)] (**2**), containing two bridging allyl ligands and one bridging allyl ligand and one bridging chloride ligand, respectively, were synthesized. The electronic structures of these complexes were investigated by combining electrospray mass spectrometry with gas phase photodetachment photoelectron spectroscopy. The major difference between the photoelectron spectra of the anions of **1** and **2** is the presence of a low-energy detachment band with an adiabatic electron detachment energy of 2.44(6) eV in **1**, which is not present in **2**. The latter has a much higher adiabatic electron detachment energy of 3.24(6) eV. Density functional theory calculations suggest that this band is present in **1** due to electron detachment from the out-of-phase combination of the π_2 orbitals, which are localized on the terminal carbon atoms of the bridging allyl ligands. In **2**, the Pd centers stabilize the single π_2 orbital of the bridging allyl ligand, and it is lowered in energy. The presence of the high-energy out-of-phase combination of the π_2 allyl orbitals makes **1** a better nucleophile, which explains why species with two bridging allyl ligands react with CO$_2$ in an analogous fashion to momoneric Pd η^1-allyls, whereas species with one bridging allyl and one bridging chloride ligand are unreactive.

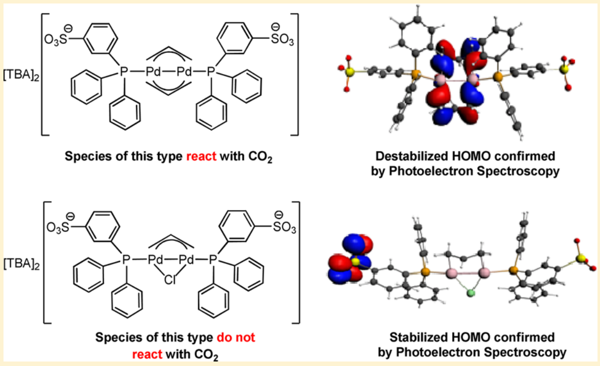

INTRODUCTION

Monomeric complexes containing a Pd allyl moiety are crucial intermediates in a wide variety of important organic reactions.[1] It is generally accepted that monomeric Pd^{II} complexes containing η^1-allyls are nucleophilic and react with electrophiles, whereas monomeric Pd^{II} complexes containing η^3-allyls are electrophilic and react with nucleophiles. In contrast, although a number of Pd^I dimers containing bridging allyl ligands have been synthesized,[2] their chemistry is less thoroughly understood. In the last 10 years several studies have been performed that indicate that Pd^I dimers containing bridging allyl ligands may also have important roles in organic transformations.

In 2004, Milstein and co-workers demonstrated that Pd^I dimers containing one bridging allyl ligand and one bridging chloride ligand were active precatalysts for the Suzuki–Miyaura reaction.[3] Subsequently, Moore reported that a related species is an efficient precatalyst for the Sonogashira coupling,[4] while Colacot also utilized a Pd^I dimer containing one bridging allyl ligand and one bridging chloride ligand for α-arylation and Buchwald–Hartwig amination reactions using aryl bromides and chlorides.[5] Furthermore, Pd^I dimers with bridging allyl ligands have also been implicated in allylic substitution reactions by Pfaltz and co-workers.[6] As part of the Hazari group's ongoing research to develop homogeneous transition metal catalysts for CO$_2$ incorporation into organic molecules,[7] we recently described unusual Pd^I dimers supported by two bridging allyl ligands (**I**) that were catalysts for the carboxylation of allylstannanes and allylboranes under mild conditions.[2d,8] The first step in the catalytic cycle is the insertion of CO$_2$ into one bridging allyl ligand to form a species with a bridging carboxlyate ligand (eq 1).[8,9] Whereas species containing two bridging allyl ligands underwent facile CO$_2$ insertion, species containing one bridging allyl ligand and one bridging chloride ligand (**II**) did not react with CO$_2$ and are catalytically inactive (eq 2).

Density functional theory (DFT) calculations showed that the nature of the HOMO was different between type **I** and type **II** complexes.[9] For type **I** systems, the highest occupied molecular orbital (HOMO) was calculated to be located almost entirely on the terminal carbon atoms of the bridging allyl

Received: October 12, 2012
Published: December 12, 2012

dx.doi.org/10.1021/om300956g | *Organometallics* 2012, 31, 8571–8576

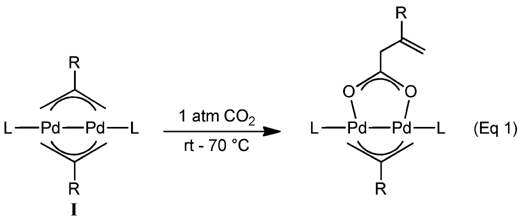

I
R = H or Me
L = PR$_3$ or NHC

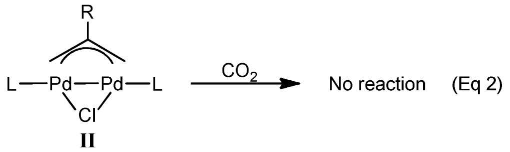

II
R = H or Me
L = PR$_3$ or NHC

ligands, whereas for type **II** species the HOMO is primarily Pd based. The HOMO of type **I** systems was calculated to be significantly higher in energy, and we proposed that this helped to facilitate the insertion of CO_2.[9] However, there was no experimental evidence to support our hypothesis of a destabilized HOMO in type **I** complexes.

Photoelectron spectroscopy (PES) has often been used to validate the calculated electronic structures of molecules in the gas phase.[10] One of the features of PES, which has limited the range of molecules that can be studied, is the need for neutral molecules to be volatile so that they can be sublimed into the gas phase. Over the past decade, the Wang group has demonstrated that by combining electrospray mass spectrometry with PES the electronic structures of a wide variety of solution anionic species, which do not sublime, can be studied in the gas phase.[11] To date, this technique has been used to successfully probe the electronic structure of many different systems, including anionic coordination compounds,[12] Fe–S clusters,[13] and, in particular, multiply charged anions.[11a,14] In this work, we have synthesized the Pd^I bridging allyl dimers **1** and **2**, which contain anionic phosphine ligands and can be considered as models for type **I** and **II** complexes, respectively. The photoelectron spectra of the anions of **1** and **2** have been recorded and show that there is a low-energy detachment present in **1**, which is absent in **2**. The relevance of this result to the insertion of CO_2 into complexes containing bridging allyl ligands is discussed.

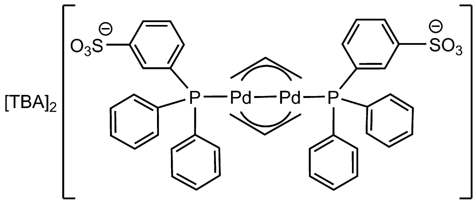

1

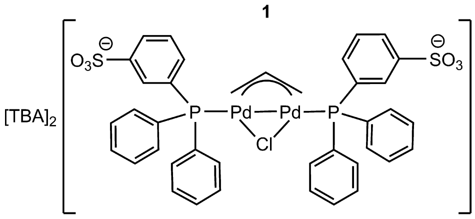

2

TBA = tetra-butylammonium

RESULTS AND DISCUSSION

Scheme 1

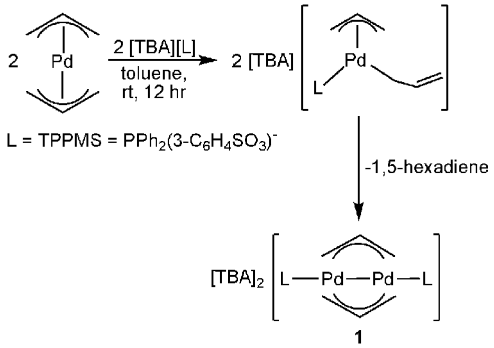

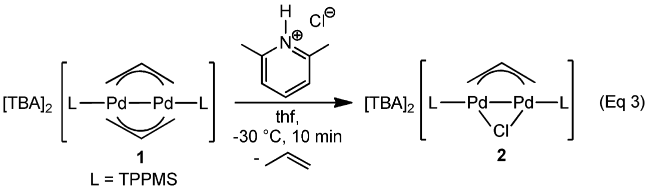

Synthesis and Characterization. Complexes **1** and **2** were prepared following the synthetic routes shown in Scheme 1 and eq 3, respectively. The Na salt of the anionic phosphine ligand TPPMS (TPPMS = $PPh_2(3\text{-}C_6H_4SO_3)^-$) was purchased from a commercial source. The Na cation was then replaced with tetrabutylammonium (TBA) by stirring [Na][TPPMS] with [TBA][Cl] in tetrahydrofuran (thf) and filtering away the NaCl precipitate. The TBA salt of TPPMS provided greater solubility for both the free ligand and the resulting complexes in organic solvents. Subsequently, reaction of [TBA][TPPMS] with (η^3-allyl)$_2$Pd in toluene at room temperature generated **1** in high yield. Both the Hazari group and others have previously used this route to generate Pd^I dimers with bridging allyl ligands, and the presence of the anionic ligand did not appear to affect the synthesis.[8,15] When the reaction was tracked using ^{1}H NMR spectroscopy, an uncharacterized intermediate, presumably the monomeric species [TBA][(η^1-allyl)(η^3-allyl)Pd(TPPMS)], was observed initially, while 1,5-hexadiene was subsequently observed as a byproduct, consistent with our previous results.[8,15] The bridging chloride salt **2** was prepared through the reaction of **1** with one equivalent of the HCl surrogate 2,6-lutidinium chloride in thf.[16] This reagent is considerably easier to use and provides cleaner reactivity than anhydrous sources of HCl in solution, which have previously been used for this type of reaction.[2a,8] The new complexes **1** and **2** were characterized by mass spectrometry, ^{1}H, ^{13}C, and ^{31}P NMR spectroscopy, and elemental analysis. They have similar spectroscopic features to other bridging allyl dimers that we have reported[8,9] but are insoluble in all hydrocarbon solvents and also diethyl ether. Both **1** and **2** are soluble in thf, acetonitrile, and dichloromethane but slow decomposition to a variety of unidentified products is observed in acetonitrile and dichloromethane at room temperature.

Photoelectron Spectroscopy of 1 and 2. The photoelectron spectra were obtained by electrospray ionization of 1 mM solutions of **1** and **2** in a thf/acetonitrile (3:1) mixed solvent. Details of the electrospray-PES apparatus have been described elsewhere.[17] Anions from the electrospray source were first accumulated in a room-temperature ion trap and then analyzed by time-of-flight mass spectrometry. The dianions of **1** and **2** were selected by a mass gate and decelerated before being photodetached by a laser beam ($h\nu$). In the current work, three laser systems were used: 355 nm (3.496 eV) and 266 nm (4.661 eV) from a Nd:YAG laser, 213 nm (5.821 eV) from a dye laser, and 157 nm (7.866 eV) from an F_2 excimer laser. In addition, we performed experiments at 266 nm for cold anions using a newly built cryogenic ion trap operated at 4.4 K.[18] The photoelectron spectra of the anion of **1** at 355 nm, 266 nm (room temperature and 4.4 K), and 157 nm are shown in Figure 1. The spectra reveal many congested detachment features, which are labeled with letters (X, A–E). These features are all fairly broad, owing to a large geometric change from the dianion to the monoanion states and/or overlaps of multiple detachment transitions. Thus, the spectral features are labeled for the sake of discussion and cannot be viewed as necessarily representing individual electronic transitions. Due to the repulsive Coulomb barrier (RCB) expected for a dianion,[14] there is a cutoff on the high binding energy side (low kinetic energy) at each photon energy. In addition, because of electron tunneling near the barriers,[19] PES features at the cutoff do not reflect the true Franck–Condon envelopes. At 355 nm (Figure 1a), band A is completely cut off due to the RCB, whereas band B is cut off in the 266 nm spectrum (Figure 1b). There is also a clear cutoff around 7 eV in the 157 nm spectrum (Figure 1c). With the consistent sharp cutoff in the spectra at the three photon energies, we estimate the magnitude of the RCB ($h\nu$ − cutoff) to be approximately 0.8 eV, which represents the intramolecular Coulomb repulsion in the parent dianion.

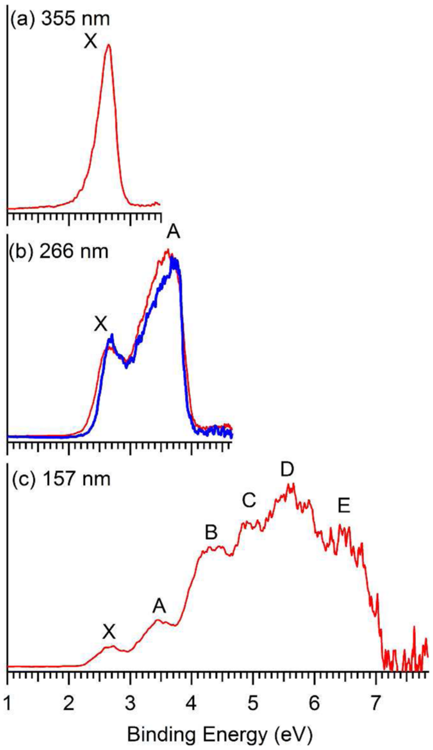

Figure 1. Photoelectron spectra of the anion of **1** at RT (red) and 4.4 K (blue): (a) 355 nm, (b) 266 nm, and (c) 157 nm.

The adiabatic (ADE) and vertical (VDE) detachment energies for band X can be determined better from the 266 nm spectrum at 4.4 K (Figure 1b) because this band should not be affected by the repulsive Coulomb barrier at this wavelength. At low temperature, vibrational hot bands were reduced, resulting in sharper onset at the low binding energy side. Because no vibrational structures were resolved, the ADE was estimated by drawing a straight line along the leading edge of the X band and then adding the instrumental resolution to the intersection with the binding energy axis. The ADE obtained for **1** is 2.44 ± 0.06 eV. The VDE was measured from the maximum of band X as 2.68 ± 0.03 eV. The ADE and VDE of **1** are given in Table 1.

Table 1. Observed and Calculated Adiabatic Electron Detachment Energies (ADE) and Vertical Electron Detachment Energies (VDE) of the First Detachment Band from the Photoelectron Spectra of 1 and 2 (all values in eV)

	exptl[a]		DFT
	ADE	VDE	VDE
1	2.44(6)	2.68(3)	2.48
2	3.24(6)	~3.5	2.82

[a]Numbers in parentheses represent the experimental uncertainties in the last digit.

The photoelectron spectra of the anion of **2** at 266 nm (room temperature and 4.4 K), 213 nm, and 157 nm are shown in Figure 2. The 157 nm spectrum (Figure 2c) shows similar detachment features to that of **1**, except for the absence of the lowest detachment band X at 2.5 eV. As for **1**, all detachment features were labeled with letters (X, A–D), but should not be viewed as representing individual electronic transitions

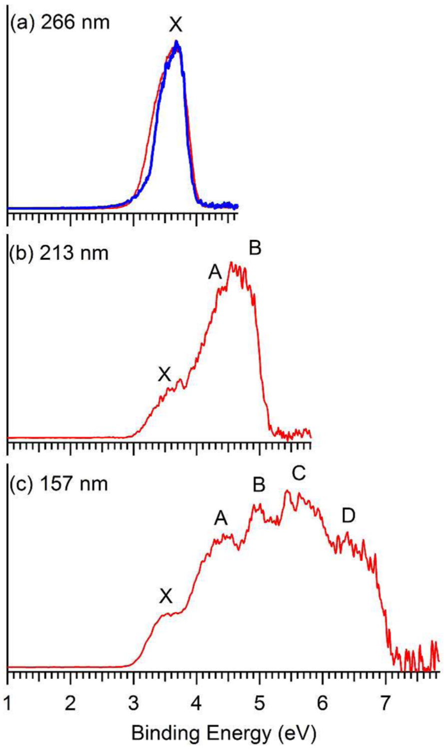

Figure 2. Photoelectron spectra of the anion of **2** at RT (red) and 4.4 K (blue): (a) 266 nm, (b) 213 nm, and (c) 157 nm.

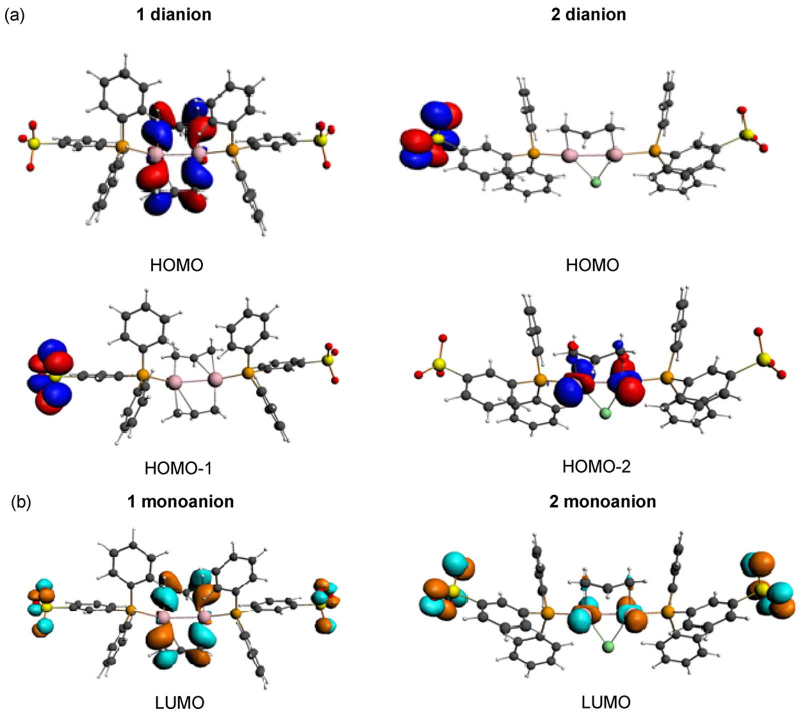

Figure 3. (a) Selected molecular orbitals of the dianions **1** and **2** and (b) the LUMOs of the monoanions of **1** and **2**.

necessarily. At lower photon energies (Figure 2a and b), we again observe spectral cutoffs due to the RCB. The estimated RCB height for **2** is also about 0.8 eV, which is reasonable because the two dianions of **1** and **2** have similar sizes. The 266 nm spectrum of **2** at 4.4 K also shows clear improvement relative to the room-temperature spectrum. Most importantly, the 4.4 K spectrum suggests that the broad band X for **2** contains multiple overlapping detachment transitions, making it difficult to determine the VDE. This observation is borne out from our calculations because near the HOMO of **2** there are close-lying O 2p lone pairs from the SO_3 groups (*vide infra*). The ADE of **2** was measured from the threshold of the 266 nm spectrum at 4.4 K to be 3.24 ± 0.06 eV. The first VDE could only be estimated to be ~3.5 eV due to the congested detachment features. These values are also given in Table 1. Overall, our PES spectra clearly show that a low-energy detachment feature is present in **1**, but not in **2**.

Density Functional Theory Analysis. The PES results clearly demonstrate that it is easier to remove an electron from **1** than **2**, thus implying that **1** is more nucleophilic. In order to understand and assign the PES spectra, and to ascertain whether the lower electron detachment energy of **1** is associated with the previously calculated HOMO of systems of type **I**, DFT calculations were performed. Initially the geometries of the $S = 0$ dianions **1** and **2** were optimized using QMMM, with the phenyl groups of the phosphine modeled at the MM level and the rest of the molecule at the QM level. Further optimization was then carried out at the QM level. For **1**, the HOMO is the same as that of related neutral compounds, consisting of the out-of-phase combination of the π_2 orbitals of the two bridging allyl ligands (Figure 3a). It is localized on the four terminal carbons of the bridging allyl ligands. The HOMO−1 and HOMO−2 are located on the SO_3 groups. The O 2p orbitals are out of phase in the familiar a_2 linear combination in the local C_{3v} symmetry of the SO_3 group (Figure 3a). Below that the orbitals resemble those of the related neutral compounds that we have previously studied.[9] The next nine orbitals in the manifold (HOMO−3 to HOMO−11) are predominantly centered on the two Pd atoms, which is consistent with two Pd^I centers, with a metal−metal single bond.

For **2**, the HOMO and HOMO−1 are localized on the SO_3 groups, consistent with the observation of overlapping detachment transitions in the 266 nm spectrum of **2** at 4.4 K. The π_2 orbital of the bridging allyl ligand is used for bonding to the metal centers in **2**, and as a result, it is stabilized and is low in the energy manifold. Instead the nine orbitals, which represent the linear combination of the two Pd centers, compose the HOMO−2 to HOMO−10. These orbitals are analogous to the HOMO to HOMO−8 in neutral type **II** systems.[9] Thus apart from the HOMO in **1**, the electronic structures of **1** and **2** are almost identical.

The electronic structures of the monoanions of **1** and **2** were then calculated, with the structures optimized for the dianions, in order to obtain vertical electron detachment energies. Values of 2.48 and 2.82 eV were found (Table 1), in reasonable agreement with the experimental findings. The associated LUMOs of the monoanions of **1** and **2** are shown in Figure 3b. In both cases the hole in the electronic structure is spread over the HOMO, HOMO−1, and HOMO−2 of the corresponding dianion, indicating that charge transfer between the SO_3 groups and the third orbital occurs on electron detachment. The hole localization is concentrated on the allyl groups in **1** and the SO_3 groups in **2**. The reason that the calculations underestimate the difference in the first detachment band between **1** and **2** is probably that the calculations overestimate the extent of hole delocalization in the monoanions. Overall, the higher energy, allyl-localized electrons are responsible for the lower electron detachment energy of **1**. In the absence of the SO_3 groups the difference between **1** and **2** would be enhanced.

CONCLUSIONS

We have prepared dianionic Pd^{I} dimers with two bridging allyl ligands and one bridging allyl ligand and one bridging chloride ligand, supported by the phosphine ligand TPPMS. The PES spectra of the anions of these compounds reveal that a low-energy electron detachment feature is present in the species with two bridging allyl ligands. DFT calculations indicate that this low-energy band occurs due to the out-of-phase combination of the π_2 orbitals of the two bridging allyl ligands. This orbital is not present in the complex with one bridging allyl and one bridging chloride ligand. The presence of the low-energy detachment band in **1** and not **2** is consistent with our proposal for why neutral complexes with two bridging allyl ligands are active catalysts for the carboxylation of allylstannanes and allylboranes, whereas species with one bridging allyl and one bridging chloride ligand do not react with CO_2 at all. It also supports our hypothesis that complexes with two bridging allyl ligands are nucleophilic, in a similar fashion to η^1-allyl moieties in Pd monomers. Furthermore, our results indicate that the PES spectra of transition metal complexes with anionic ligands can be used as models for investigating the electronic structure of neutral complexes. In the future, we will look to extend our work to obtain the PES spectra of the anions of other nonvolatile organometallic complexes, which are relevant to CO_2 conversion.

EXPERIMENTAL SECTION

General Methods. Experiments were performed under a dinitrogen atmosphere in an M-Braun drybox or using standard Schlenk techniques. (Under standard glovebox conditions purging was not performed between uses of pentane, diethyl ether, benzene, toluene, and thf; thus when any of these solvents were used, traces of all these solvents were in the atmosphere and could be found intermixed in the solvent bottles.) Moisture- and air-sensitive liquids were transferred by stainless steel cannula on a Schlenk line or in a drybox. The solvents for air- and moisture-sensitive reactions were dried by passage through a column of activated alumina followed by storage under dinitrogen. All commercial chemicals were used as received except where noted. Deuterated solvents were obtained from Cambridge Isotope Laboratories. Both CD_2Cl_2 and CD_3CN were dried over calcium hydride and distilled prior to use. NMR spectra were recorded on Bruker AMX-400 or -500 spectrometers at ambient probe temperatures unless noted. Chemical shifts are reported with respect to residual internal protio solvent for ^{1}H and $^{13}C\{^{1}H\}$ NMR spectra and to an external standard for $^{31}P\{^{1}H\}$ spectra (85% H_3PO_4 at 0.0 ppm). Robertson Microlit Laboratories, Inc. performed the elemental analyses (inert atmosphere). The low %C observed in the analyses are typical for Pd^{I} dimers with bridging allyl ligands.[8,9] Literature procedures were followed to prepare the following compounds: (η^3-allyl)$_2$Pd[20] and 2,6-lutidinium chloride.[16]

Electrospray and PES Spectroscopy. Experiments were carried out using the electrospray ionization PES (ESI-PES) apparatus, which has been described previously in detail.[17] The only modification was the shortening of the electron flight tube from 4.0 m to 2.5 m, leading to only a slight decrease of electron energy resolution.[21] The dianions of the Pd dimer **1** or **2** were produced by electrospray ionization of a 1 mM solution of the corresponding TBA salts from a mixed thf/acetonitrile (3:1) solution. Upon exposure to air during electrospray ionization, compound **1** started to decompose, and therefore N_2 gas was used to purge the ESI zone to minimize the air contamination and enhance the mass signals. A radio frequency-only quadrupole device guided the anions from the ESI source into a Paul trap operated at room temperature, where anions were accumulated for 0.1 s before being pulsed into the extraction zone of a time-of-flight mass spectrometer. The anions of interest were selected by a mass gate and decelerated before being intercepted by a laser beam in the detachment region of a magnetic-bottle photoelectron analyzer. In the current work, three different lasers were used for the PES experiment: 157 nm (7.866 eV) from an F_2 excimer laser, 213 nm (5.821 eV) from a dye laser, and 266 nm (4.661 eV) and 355 nm (3.496 eV) from a Nd:YAG laser. At 266 nm, we improved the energy resolution of the PES spectra of both species by using our newly built cryogenic ion trap[18,22] operated at 4.4 K. The PES spectra were calibrated using the known spectra of Au^- and I^-. The Au^- anion was produced by electrospray ionization of a pyridine solution of PPh_3AuCl with $NaSCH_3$ and a trace amount of CH_3OH.[23] The electron kinetic energy resolution of the current magnetic-bottle photoelectron analyzer with the shortened electron flight tube was about 3%, i.e., 30 meV for 1 eV electrons.[21]

DFT Calculations. Quantum chemical calculations were performed using density functional methods of the Amsterdam Density Functional (Version ADF2011.02) package.[24] TZP basis sets were used with triple-ξ accuracy sets of Slater-type orbitals, with polarization functions added to all atoms. Relativistic corrections were made using the ZORA (zero-order relativistic approximation) formalism, and the core electrons were frozen up to 1s for C and O, 2p for P and S, and 3d for Pd. The B3LYP functional was used.[25] The geometries of the dianions of **1** and **2** were optimized, and the optimized structure was used to estimate vertical electron detachment energies for the monoanions. The Kohn–Sham orbitals of the dianions were used as the basis sets for the respective monoanion calculations to assist with SCF convergence.

Synthesis and Characterization of Compounds. *[TBA][TPPMS].* Sodium triphenylphosphine-*meta*-sulfonate (137 mg, 0.37 mmol) and tetrabutylammonium chloride (104 mg, 0.37 mmol) were dissolved in 5 mL of thf. The reaction was stirred for 30 min at room temperature. After this time a white precipitate had formed, and the filtrate was isolated by cannular filtration. The volatiles were removed under reduced pressure to give a white solid. The solid was dissolved in a minimal amount of toluene, and then pentane was added until a precipitate formed. The solvent was decanted, and the precipitate was washed with pentane (3 × 3 mL). The residual solvent was then removed under reduced pressure to leave [TBA][TPPMS] as a white powder (164 mg, 75%).

[TBA]$_2$[(TPPMS)$_2$Pd$_2$(μ-C_3H_5)$_2$] **(1)**. In a 22 mL vial with a stir bar, (η^3-allyl)$_2$Pd (29 mg, 0.15 mmol) and [TBA][TPPMS] (89 mg, 0.15 mmol) were dissolved in 4 mL of toluene. The reaction was stirred for 12 h at room temperature. After this time a yellow powder had precipitated out of solution. The solvent was carefully decanted from the solid, and the yellow residue was washed with toluene (3 × 3 mL) and dried *in vacuo*. The resulting solid was triturated with pentane (3 × 5 mL), and the solid was dried under reduced pressure to give **1** (104 mg, 94%) as a bright yellow powder.
ESI-MS (1:1 thf/acetonitrile) m/z: 489 $[M]^{2-}$. ^{1}H NMR (500 MHz, CD_3CN): δ 7.77 (d, J = 7.3 Hz, 2H, H_{Ar}), 7.74 (s, 2H, H_{Ar}), 7.48–7.30 (m, 24H, H_{Ar}), 3.66 (m, 2H, allyl-central), 3.08 (m, 16H, Bu_4N NCH_2), 2.07 (d, J = 6.9 Hz, 4H, allyl-end), 1.58 (m, 16H, Bu_4N NCH_2CH_2), 1.39 (d, J = 12.8 Hz, 4H, allyl-end), 1.32 (m, 16H, Bu_4N $NCH_2CH_2CH_2$), 0.94 (t, J = 7.4 Hz, 24H, Bu_4N CH_3). $^{13}C\{^{1}H\}$ NMR (126 MHz, CD_3CN): δ 148.7 (t, J = 3.4 Hz), 136.0–135.7 (m), 134.5 (t, J = 6.8 Hz), 130.8 (t, J = 6.4 Hz), 128.6 (t, J = 4.5 Hz), 128.2 (t, J = 4.6 Hz), 127.7, 93.8, 59.3, 35.2, 24.3, 20.3, 13.8. $^{31}P\{^{1}H\}$ NMR (121 MHz, CD_3CN): δ 32.66. Anal. Calcd (found) for $C_{74}H_{110}N_2O_6P_2Pd_2S_2$: C, 60.77 (59.55); H, 7.58 (7.41); N, 1.92 (2.04).

[TBA]$_2$[(TPPMS)$_2$Pd$_2$(μ-C_3H_5)(μ-Cl)] **(2)**. Compound **1** (49 mg, 0.034 mmol) and 2,6-lutidinium chloride (4.8 mg, 0.034 mmol) were dissolved in 5 mL of thf that had been cooled to −30 °C. After stirring at −30 °C for 10 minutes the vial was allowed to warm to room temperature. The volatiles were then removed under reduced pressure. The resultant dark yellow oil was triturated with pentane (3 × 2 mL) in a sonicator for 10 minutes. The resultant yellow residue was dried under vacuum to give **2** (40 mg, 81%) as a bright yellow powder.
ESI-MS (1:1 thf/acetonitrile) m/z: 486 $[M - Cl]^{2-}$. ^{1}H NMR (400 MHz, CD_2Cl_2): δ 7.91 (br, 2H, H_{Ar}), 7.86 (d, J = 7.7 Hz, 2H, H_{Ar}), 7.72 (br, 4H, H_{Ar}), 7.63 (br, 4H, H_{Ar}), 7.53 (d, J = 5.7 Hz, 2H, H_{Ar}),

7.47−7.33 (br m, 13H, H_{Ar}), 3.13 (t, J = 8.4 Hz, 16 H, $Bu_4N\ NCH_2$), 2.90 (d, J = 6.5 Hz, 2H, allyl-end), 2.81 (m, 1H, allyl-central), 1.54 (t, J = 8.0 Hz, 16H, $Bu_4N\ NCH_2CH_2$), 1.45 (d, J = 12.7 Hz, 2H, allyl-end) 1.30 (q, J = 7.4 Hz, 16H, $Bu_4N\ NCH_2CH_2CH_2$), 0.91 (t, J = 7.3 Hz, 24H, $Bu_4N\ CH_3$). $^{13}C\{^1H\}$ NMR (126 MHz, CD_3CN): δ 149.10 (t, J = 4.2 Hz), 134.8−135.2 (m), 134.8−134.6 (m), 134.5, 130.9 (t, J = 7.4 Hz), 130.4, 130.3, 139.0 (q, J = 4.8 Hz), 128.6 (t, J = 4.7 Hz), 128.2, 73.4, 59.3, 41.6, 24.4, 20.2, 14.0. $^{31}P\{^1H\}$ NMR (121 MHz, CD_2Cl_2): δ 27.12. Anal. Calcd (found) for $C_{71}H_{105}ClN_2O_6P_2Pd_2S_2$: C, 58.53 (56.51); H, 7.26 (7.05); N, 1.92 (1.92).

■ ASSOCIATED CONTENT

Ⓢ Supporting Information

Further information about DFT calculations, including xyz files for optimized structures, is available free of charge via the Internet at http://pubs.acs.org.

■ AUTHOR INFORMATION

Corresponding Author

*E-mail: jennifer.green@chem.ox.ac.uk; nilay.hazari@yale.edu; lai-sheng_wang@brown.edu.

Author Contributions

‡These authors contributed equally.

Notes

The authors declare no competing financial interest.

■ ACKNOWLEDGMENTS

L.S.W. thanks the National Science Foundation (CHE-1049717) for support of this research. N.H. gratefully acknowledges support through a Doctoral New Investigator Grant from the ACS Petroleum Research Fund (51009-DNI3). D.P.H. thanks the NSF for support as an NSF Graduate Research Fellow, and M.J.C. thanks Yale College for funding as part of the Yale Science Scholars Program.

■ REFERENCES

(1) (a) Tsuji, J. *Perspectives in Organopalladium Chemistry for the 21st Century*; Elsevier: Amsterdam, 1999. (b) Tsuji, J. *Palladium Reagents and Catalysis: Innovations in Organic Synthesis*; Wiley: Chichester, 1995. (c) Negishi, E.; de Meijre, A. *Organopalladium Chemistry for Organic Synthesis*; Wiley: New York, 2002; Vol. 2.

(2) (a) Werner, H. *Adv. Organomet. Chem.* **1981**, *19*, 155. (b) Murahashi, T.; Kurosawa, H. *Coord. Chem. Rev.* **2002**, *231*, 207. (c) Kurosawa, H. *J. Organomet. Chem.* **2004**, *689*, 4511. (d) Hazari, N.; Hruszkewycz, D. P.; Wu, J. *Synlett* **2011**, 1793.

(3) Weissman, H.; Shimon, L. J. W.; Milstein, D. *Organometallics* **2004**, *23*, 3931.

(4) Elliott, E. L.; Ray, C. R.; Kraft, S.; Atkins, J. R.; Moore, J. S. *J. Org. Chem.* **2006**, *71*, 5282.

(5) Hill, L. L.; Crowell, J. L.; Tutwiler, S. L.; Massie, N. L.; Hines, C. C.; Griffin, S. T.; Rogers, R. D.; Shaughnessy, K. H.; Grasa, G. A.; Johansson Seechurn, C. C. C.; Li, H.; Colacot, T. J.; Chou, J.; Woltermann, C. J. *J. Org. Chem.* **2010**, *75*, 6477.

(6) Markert, C.; Neuburger, M.; Kulicke, K.; Meuwly, M.; Pfaltz, A. *Angew. Chem., Int. Ed.* **2007**, *46*, 5892.

(7) (a) Wu, J.; Green, J. C.; Hazari, N.; Hruszkewycz, D. P.; Incarvito, C. D.; Schmeier, T. J. *Organometallics* **2010**, *29*, 6369. (b) Wu, J.; Hazari, N. *Chem. Commun.* **2011**, *47*, 1069. (c) Wu, J.; Hazari, N.; Incarvito, C. D. *Organometallics* **2011**, *30*, 3142. (d) Schmeier, T. J.; Hazari, N.; Incarvito, C. D.; Raskatov, J. R. *Chem. Commun.* **2011**, *47*, 1824. (e) Schmeier, T. J.; Nova, A.; Hazari, N.; Maseras, F. *Chem.—Eur. J.* **2012**, *18*, 6915.

(8) Hruszkewycz, D. P.; Wu, J.; Hazari, N.; Incarvito, C. D. *J. Am. Chem. Soc.* **2011**, *133*, 3280.

(9) Hruszkewycz, D. P.; Wu, J.; Green, J. C.; Hazari, N.; Schmeier, T. J. *Organometallics* **2012**, *31*, 470.

(10) (a) Green, J. C. *Acc. Chem. Res.* **1994**, *27*, 131. (b) Green, J. C. In *Comprehensive Organometallic Chemistry III*; Crabtree, R. H., Mingos, D. M. P., Eds.; Elsevier: Oxford, 2007; Vol. *1*, pp 381−406. (c) Gruhn, N. E.; Lichtenberger, D. L. *Photoelectron Spectroscopy* from 'Applications of Physical Methods to Inorganic and Bioinorganic Chemistry'; Scott, R. A.; Lukehart, C. M., Eds.; Wiley: West Sussex, UK, 2007; pp 441−459.

(11) (a) Wang, L. S.; Wang, X. B. *J. Phys. Chem. A* **2000**, *104*, 1978. (b) Wang, X. B.; Yang, X.; Wang, L. S. *Int. Rev. Phys. Chem.* **2002**, *21*, 473.

(12) (a) Wang, X. B.; Wang, L. S. *J. Chem. Phys.* **1999**, *111*, 4497. (b) Waters, T.; Woo, H. K.; Wang, X. B.; Wang, L. S. *J. Am. Chem. Soc.* **2006**, *128*, 4282.

(13) (a) Wang, X. B.; Niu, S.; Yang, X.; Ibrahim, S. K.; Pickett, C. J.; Ichiye, T.; Wang, L. S. *J. Am. Chem. Soc.* **2003**, *125*, 14072. (b) Yang, X.; Niu, S.; Ichiye, T.; Wang, L. S. *J. Am. Chem. Soc.* **2004**, *126*, 15790. (c) Tard, C.; Liu, X.; Ibrahim, S. K.; Bruschi, M.; De Gioia, L.; Davies, S. C.; Yang, X.; Wang, L. S.; Sawers, G.; Pickett, C. J. *Nature* **2005**, *433*, 610.

(14) (a) Wang, L. S.; Ding, C. F.; Wang, X. B.; Nicholas, J. B. *Phys. Rev. Lett.* **1998**, *81*, 2667. (b) Wang, X. B.; Wang, L. S. *Nature* **1999**, *400*, 245.

(15) (a) Benn, R.; Jolly, P. W.; Mynott, R.; Raspel, B.; Schenker, G.; Schick, K. P.; Schroth, G. *Organometallics* **1985**, *4*, 1945. (b) Krause, J.; Goddard, R.; Mynott, R.; Pörschke, K.-R. *Organometallics* **2001**, *20*, 1992.

(16) (a) Grönberg, K. L. C.; Henderson, R. A.; Oglieve, K. E. *J. Chem. Soc., Dalton Trans.* **1998**, 3093. (b) Garratt, S. A.; Hughes, R. P.; Kovacik, I.; Ward, A. J.; Willemsen, S.; Zhang, D. *J. Am. Chem. Soc.* **2005**, *127*, 15585.

(17) Wang, L. S.; Ding, C. F.; Wang, X. B.; Barlow, S. E. *Rev. Sci. Instrum.* **1999**, *70*, 1957.

(18) (a) Wang, X. B.; Wang, L. S. *Rev. Sci. Instrum.* **2008**, *79*, 073108/1. (b) Dau, P. D.; Liu, H. T.; Huang, D. L.; Wang, L. S. *J. Chem. Phys.* **2012**, *137*, 116101/1.

(19) Wang, X. B.; Ding, C. F.; Wang, L. S. *Chem. Phys. Lett.* **1999**, *307*, 391.

(20) Goliaszewski, A.; Schwartz, J. *Tetrahedron* **1985**, *41*, 5779.

(21) Liu, H. T.; Wang, Y. L.; Xiong, X. G.; Dau, P. D.; Piazza, Z.; Huang, D. L.; Xu, C. Q.; Li, J.; Wang, L. S. *Chem. Sci.* **2012**, *3*, 3286.

(22) Liu, H. T.; Dau, P. D.; Huang, D. L.; Wang, L. S. *Rev. Sci. Intrum.* To be published.

(23) Ning, C. G.; Xiong, X. G.; Wang, Y. L.; Li, J.; Wang, L. S. *Phys. Chem. Chem. Phys.* **2012**, *14*, 9323.

(24) (a) Baerends, E. J.; Ellis, D. E.; Ros, P. *Chem. Phys.* **1973**, *2*, 41. (b) Versluis, L.; Ziegler, T. *J. Chem. Phys.* **1988**, *88*, 322. (c) Fonseca Guerra, C.; Snijder, J. G.; te Velde, G.; Baerends, E. J. *Theor. Chem. Acc.* **1998**, *99*, 391. (d) te Velde, G.; Bickelhaupt, F. M.; Baerends, E. J.; Fonseca Guerra, C.; Van Gisbergen, S. J. A.; Snijders, J. G.; Ziegler, T. *J. Comput. Chem.* **2001**, *22*, 931. (e) *ADF2012*; SCM, Theoretical Chemistry, Vrije Universiteit: Amsterdam, The Netherlands, http://www.scm.com.

(25) Stephens, P. J.; Devlin, F. J.; Chabalowski, C. F.; Frisch, M. J. *J. Phys. Chem.* **1994**, *98*, 11623.